(Received 12 October 2023, Accepted 3 July 2024, Scheduled 10 July 2024)

Separating the Bulk and Surface Second Harmonic Quadrupolar Contribution in Inversion Symmetric Crystals

Damián Zúñiga-Avelar[1], Omar Palillero-Sandoval[1], Rosibel Carrada-Legaria[2], Muhammad Ahyad[3], Hendradi Hardhienata[3], and Adalberto Alejo-Molina[4,*]

[1]*Instituto de Investigación en Ciencias Básicas y Aplicadas (IICBA), UAEM Cuernavaca, Mor. 62160, México*
[2]*Facultad de Ciencias Físico-Matemáticas, BUAP, Av. San Claudio, Puebla, Pue. 72570, México*
[3]*Theoretical Physics Division, Department of Physics, Bogor Agricultural University Meranti Avenue, Wing S Building, Dramaga Campus of IPB, Bogor 16680, West Java, Indonesia*
[4]*CONAHCYT — Instituto de Investigación en Ciencias Básicas y Aplicadas (IICBA), UAEM Cuernavaca, Mor. 62160, México*

ABSTRACT: We apply the third-order susceptibility tensor generated by the Simplified Bond Hyperpolarizability Model (SBHM) to address the long standing challenges in distinguishing the bulk and surface quadrupolar second-harmonic-generation (SHG) contributions in diamond lattices, such as silicon, which exhibit bulk inversion symmetry. Assuming that the quadrupolar contribution originates from the interface gradient of the excited electric field, we demonstrate through symmetry considerations and numerical calculations for Si(001) and Si(111) facet orientations that it is not possible to separate the different quadrupolar contributions when the incoming light is incident normally. However, we show that such separation is achievable with oblique incidence. Furthermore, we propose a novel experimental design to measure the bulk and surface quadrupolar SHG contributions separately by introducing a semi-vicinal surface. Using numerical SBHM simulations, we show for the first time that this semi-vicinal setup can prove the existence of spatial dispersion, a nonlinear dipolar bulk effect recently proposed. This approach may lead to a better understanding of various nonlinear contributions in silicon and enable precise nonlinear surface monitoring.

1. INTRODUCTION

It is commonly accepted that the research in nonlinear optics (NLO) began to flourish following the observation of second-harmonic generation (SHG) by Franken et al. [1], just several months after Maiman discovered the laser [2]. Theoretical work in SHG soon followed with seminal contributions from Bloembergen and coworkers [3, 4]. Subsequently, studies on third harmonic generation were published by Maker and Terhune [5], and also by Ward and New [6], using different media. Since then, contributions to the field of nonlinear optics have grown exponentially.

Several methods for modeling SHG using bond models exist [7–9]. However, the approach for calculating the far-field contribution proposed by Aspnes and his group [10, 11], called the Simplified Bond-Hyperpolarizability Model (SBHM), has significantly simplified NLO and reproduces experimental rotational anisotropy SHG intensity very well for low symmetry crystals without surface reconstruction, terraces, or other defects. Nevertheless, it is well known that SBHM has some limitations [12]. In 2013, Hingerl and his group explored SBHM further, comparing the second-order susceptibilities obtained by the model with group theory and tensor rotations. They obtained the same susceptibility tensors found in crystallographic tables and extended the model to other high-order phenomena [13–19]. More recently, other research groups have continued working with this model to explain NLO experimental results in more complex materials and situations [20–24].

Studies on nonlinear phenomena originating from quadrupolar sources began around the same time as the explanation of harmonic generation due to dipolar contributions. Indeed, such work was published by Bloembergen and coworkers [25], where they derived expressions for the quadrupolar contribution from localized orbitals. In a more modern interpretation of nonlinear polarization, Bauer et al. [26] distinguishes between quadrupolar contributions from the electric quadrupole and the magnetic dipole moments, proposing a more general form for total nonlinear polarization. More recently, quadrupolar contributions to SHG have been studied from the viewpoint of the microscopic response function [26], the classical oscillator model [27], as well as from the perspective of SBHM.

In this work, we apply the Simplified Bond-Hyperpolarizability Model (SBHM) to discuss the issue of separating the different contributions to second-harmonic generation (SHG) in inversion-symmetric materials, such as silicon, which has a diamond structure. In inversion-symmetric materials, SHG from dipoles is forbidden due to parity symmetry. However, this symmetry is broken at the surface, so the main SHG contribution from the surface is produced by dipolar interactions, while inside the bulk, SHG is generated by quadrupolar and spatial dispersion phenomena. The latter contribution has been sufficiently discussed in [21].

* Corresponding author: Adalberto Alejo-Molina (adalberto.alejo@uaem.mx).

This manuscript is organized as follows. Section 2 provides a short but general description of the SBHM and how it can be developed to account for the gradient of the excitation electric field at the silicon interface, which generates the SHG quadrupolar contribution. In Section 3, the susceptibility fourth-rank tensor describing the quadrupolar contribution due to the gradient of the fundamental electric field is discussed for the Si(001) and Si(111) facet orientations. An effective tensor is introduced to simplify the SHG tensorial analysis of the silicon surface in the same directions. Finally, in Section 4, we provide a conclusion of our work.

2. SBHM OF SHG BULK QUADRUPOLAR CONTRIBUTION

The original Simplified Bond-Hyperpolarizability Model (SBHM) is based on three assumptions: (1) Dipoles oscillate only in the atomic bond directions; (2) the same electric field generates both a linear and nonlinear response that drives the electrons harmonically and anharmonically; and (3) there is no reconstruction on the surfaces or in the bulk. The latter means that the orientations of the bonds are the same, but the hyperpolarizabilities change if they are on the surface or in the bulk. In more recent work, SHG from wurtzite semiconductors with surface reconstructions, such as twin boundaries, has been analyzed using the SBHM with good precision [28].

SBHM is an elegant way of restating the results of the harmonic oscillator with the addition of anharmonic contributions, providing a method to calculate the susceptibilities in crystals, which are needed to determine the linear and nonlinear polarizations. It is well known that polarization can be expressed as a power series in the field strength [29].

$$\begin{aligned}
\vec{P}(\omega) &= \varepsilon_0\left\{\overleftrightarrow{\chi}^{(1)}\cdot\vec{E}(\omega)+\overleftrightarrow{\chi}^{(2A)}\cdot\cdot\left[\vec{E}(\omega)\otimes\vec{E}(0)\right]+\ldots\right\}\\
\vec{P}(2\omega) &= \varepsilon_0\left\{\overleftrightarrow{\chi}^{(2)}\cdot\cdot\left[\vec{E}(\omega)\otimes\vec{E}(\omega)\right]\right.\\
&\quad\left.+\overleftrightarrow{\chi}^{(3A)}\cdots\left[\vec{E}(\omega)\otimes\vec{E}(\omega)\otimes\vec{E}(0)\right]+\cdots\right\}\\
\vec{P}(3\omega) &= \varepsilon_0\left\{\overleftrightarrow{\chi}^{(3)}\cdots\left[\vec{E}(\omega)\otimes\vec{E}(\omega)\otimes\vec{E}(\omega)\right]+\cdots\right\}
\end{aligned} \tag{1}$$

where $\vec{P}(\omega)$ is the linear polarization, $\vec{P}(2\omega)$ the second harmonic contribution, and $\vec{P}(3\omega)$ the third harmonic contribution. Here, $\vec{E}(\omega)$ is the fundamental electric field, whereas $\overleftrightarrow{\chi}^{(1)}$ is known as the first-order susceptibility; $\overleftrightarrow{\chi}^{(2A)}$ describes the linear electro-optic (also called Kerr) effect (i.e., the modification of the dielectric function/refractive index through a DC field $\vec{E}(0)$); $\overleftrightarrow{\chi}^{(2)}$ corresponds to second harmonic generation; $\overleftrightarrow{\chi}^{(3A)}$ is the electric field induced second harmonic (EFISH) generation [18]; and finally, $\overleftrightarrow{\chi}^{(3)}$ is associated with third harmonic generation [15]. If the electric field is described in a full vectorial way, then in general $\overleftrightarrow{\chi}^{(1)}$, $\overleftrightarrow{\chi}^{(2)}$ and $\overleftrightarrow{\chi}^{(3)}$ are represented through second-, third- and fourth-rank tensors, respectively. We note that $\overleftrightarrow{\chi}^{(3A)}$ and $\overleftrightarrow{\chi}^{(3)}$ will not have the same values, but due to symmetry the same tensorial form.

In particular, the quadrupolar contribution due to the absorption of the incoming electric field inside the material is mathematically represented by the gradient of the electric field. Thus, according to the SBHM, the SHG nonlinear polarization is given by

$$\begin{aligned}
\vec{P}(2\omega) &= \overleftrightarrow{\chi}^{(3B)}\cdots\left[\vec{E}(\omega)\otimes\nabla\otimes\vec{E}(\omega)\right]\\
&= \frac{1}{V}\sum\nolimits_j\left[\alpha_{3B}\hat{b}_j\otimes\hat{b}_j\otimes\hat{b}_j\otimes\hat{b}_j\right]\\
&\quad\cdots\left[\vec{E}(\omega)\otimes\nabla\otimes\vec{E}(\omega)\right]
\end{aligned} \tag{2}$$

here comparing the two equalities in Eq. (2), it is clear that

$$\overleftrightarrow{\chi}^{(3B)} = \frac{1}{V}\sum\nolimits_j\left[\alpha_{3B}\hat{b}_j\otimes\hat{b}_j\otimes\hat{b}_j\otimes\hat{b}_j\right] \tag{3}$$

where $\overleftrightarrow{\chi}^{(3B)}$ is the susceptibility fourth-rank tensor of the third order related to SHG; the "$\hat{b}_j$s" are the unitary vectors in the direction of the atomic bonds; α_{3B} is the second order hyperpolarizability; V is the volume of the conventional cell. Moreover, Eq. (2) can be rewritten in terms of the components as:

$$P_i(2\omega) = \chi_{ijkl}E_j\nabla_k E_l \tag{4}$$

where ∇_k denotes the electric field gradient inside the material. Usually, the experimental method for determining the intensity variations of the second harmonic signal that originates from the surface is "Rotational Anisotropy Second Harmonic Generation" (RASHG). This method involves rotating the crystal around the surface normal (typically labeled as z-axis) and is denoted as the azimuthal rotating angle ϕ. In this way, the generated nonlinear intensity has an azimuthal dependence and should be included in the nonlinear polarization *via* the direct vector product of the atomic covalent bond unit vectors, as follows:

$$\begin{aligned}
\overleftrightarrow{\chi}^{(3B)} &= \frac{1}{V}\sum_{j=1}^{4}\left[\alpha_{3B}\left\{\mathbf{R}^{(z)}(\phi)\cdot\hat{b}_j\right\}\otimes\left\{\mathbf{R}^{(z)}(\phi)\cdot\hat{b}_j\right\}\right.\\
&\quad\left.\otimes\left\{\mathbf{R}^{(z)}(\phi)\cdot\hat{b}_j\right\}\otimes\left\{\mathbf{R}^{(z)}(\phi)\cdot\hat{b}_j\right\}\right]
\end{aligned} \tag{5}$$

where $\mathbf{R}^{(z)}$ is a rotation matrix around the z-axis. On the other hand, the definition of the atomic bond unit vectors depends on the crystal direction. In the next section, we will discuss these vectors for the two main facet orientations in silicon namely Si(001) and Si(111).

3. SUSCEPTIBILITY TENSORS FOR THE SHG QUADRUPOLAR CONTRIBUTION TO THE BULK

3.1. Si(001) Facet

For a Si(001) facet orientation SBHM only requires four bond unit vectors which have the following mathematical expressions [16]:

$$\hat{b}_1 = -\begin{pmatrix} \frac{\sqrt{2}}{2}\sin\frac{\beta}{2} \\ \frac{\sqrt{2}}{2}\sin\frac{\beta}{2} \\ \cos\frac{\beta}{2} \end{pmatrix}, \quad \hat{b}_2 = \begin{pmatrix} \frac{\sqrt{2}}{2}\sin\frac{\beta}{2} \\ \frac{\sqrt{2}}{2}\sin\frac{\beta}{2} \\ -\cos\frac{\beta}{2} \end{pmatrix},$$
$$\hat{b}_3 = \begin{pmatrix} -\frac{\sqrt{2}}{2}\sin\frac{\beta}{2} \\ \frac{\sqrt{2}}{2}\sin\frac{\beta}{2} \\ \cos\frac{\beta}{2} \end{pmatrix}, \quad \hat{b}_4 = \begin{pmatrix} \frac{\sqrt{2}}{2}\sin\frac{\beta}{2} \\ -\frac{\sqrt{2}}{2}\sin\frac{\beta}{2} \\ \cos\frac{\beta}{2} \end{pmatrix} \tag{6}$$

where $\beta = 2\arccos\left(\frac{1}{\sqrt{3}}\right) \approx 109.47°$, is the angle between the atomic bonds. Thus, according to Eq. (5) the susceptibility tensor for the quadrupolar contribution will be:

$$\overleftrightarrow{\chi}^{(3B)} = \frac{\alpha_{3B}}{V}$$
$$\left(\begin{pmatrix} [3+\cos(4\phi)]\sin^4\left(\frac{\beta}{2}\right) & \sin(4\phi)\sin^4\left(\frac{\beta}{2}\right) & 0 \\ \sin(4\phi)\sin^4\left(\frac{\beta}{2}\right) & 2\sin^2(2\phi)\sin^4\left(\frac{\beta}{2}\right) & 0 \\ 0 & 0 & \sin^2\beta \end{pmatrix} \begin{pmatrix} \sin(4\phi)\sin^4\left(\frac{\beta}{2}\right) & 2\sin^2(2\phi)\sin^4\left(\frac{\beta}{2}\right) & 0 \\ 2\sin^2(2\phi)\sin^4\left(\frac{\beta}{2}\right) & -\sin^2(4\phi)\sin^4\left(\frac{\beta}{2}\right) & 0 \\ 0 & 0 & 0 \end{pmatrix} \begin{pmatrix} 0 & 0 & \sin^2\beta \\ 0 & 0 & 0 \\ \sin^2\beta & 0 & 0 \end{pmatrix} \right.$$
$$\left. \begin{pmatrix} \sin(4\phi)\sin^4\left(\frac{\beta}{2}\right) & 2\sin^2(2\phi)\sin^4\left(\frac{\beta}{2}\right) & 0 \\ 2\sin^2(2\phi)\sin^4\left(\frac{\beta}{2}\right) & -\sin^2(4\phi)\sin^4\left(\frac{\beta}{2}\right) & 0 \\ 0 & 0 & 0 \end{pmatrix} \begin{pmatrix} 2\sin^2(2\phi)\sin^4\left(\frac{\beta}{2}\right) & -\sin^2(4\phi)\sin^4\left(\frac{\beta}{2}\right) & 0 \\ -\sin^2(4\phi)\sin^4\left(\frac{\beta}{2}\right) & [3+\cos(4\phi)]\sin^4\left(\frac{\beta}{2}\right) & 0 \\ 0 & 0 & \sin^2\beta \end{pmatrix} \begin{pmatrix} 0 & 0 & 0 \\ 0 & 0 & \sin^2\beta \\ 0 & \sin^2\beta & 0 \end{pmatrix} \right.$$
$$\left. \begin{pmatrix} 0 & 0 & \sin^2\beta \\ 0 & 0 & 0 \\ \sin^2\beta & 0 & 0 \end{pmatrix} \begin{pmatrix} 0 & 0 & 0 \\ 0 & 0 & \sin^2\beta \\ 0 & \sin^2\beta & 0 \end{pmatrix} \begin{pmatrix} \sin^2\beta & 0 & 0 \\ 0 & \sin^2\beta & 0 \\ 0 & 0 & 8\cos^4\left(\frac{\beta}{2}\right) \end{pmatrix} \right). \tag{7}$$

According to the SBHM, this is the general tensor describing the third order susceptibility which looks very complicated However, choosing a particular azimuthal rotation will simplify it. For example, if we evaluate the angle β and taking $\phi = \pi/4$ in Eq. (7) yields

$$\overleftrightarrow{\chi}^{(3B)} = \frac{8\alpha_{3B}}{9V}$$
$$\left(\begin{pmatrix} 1 & 0 & 0 \\ 0 & 1 & 0 \\ 0 & 0 & 1 \end{pmatrix} \begin{pmatrix} 0 & 1 & 0 \\ 1 & 0 & 0 \\ 0 & 0 & 0 \end{pmatrix} \begin{pmatrix} 0 & 0 & 1 \\ 0 & 0 & 0 \\ 1 & 0 & 0 \end{pmatrix} \right.$$
$$\left. \begin{pmatrix} 0 & 1 & 0 \\ 1 & 0 & 0 \\ 0 & 0 & 0 \end{pmatrix} \begin{pmatrix} 1 & 0 & 0 \\ 0 & 1 & 0 \\ 0 & 0 & 1 \end{pmatrix} \begin{pmatrix} 0 & 0 & 0 \\ 0 & 0 & 1 \\ 0 & 1 & 0 \end{pmatrix} \right.$$
$$\left. \begin{pmatrix} 0 & 0 & 1 \\ 0 & 0 & 0 \\ 1 & 0 & 0 \end{pmatrix} \begin{pmatrix} 0 & 0 & 0 \\ 0 & 0 & 1 \\ 0 & 1 & 0 \end{pmatrix} \begin{pmatrix} 1 & 0 & 0 \\ 0 & 1 & 0 \\ 0 & 0 & 1 \end{pmatrix} \right), \tag{8}$$

We now obtain a simplified version of the fourth-rank tensor described by only one independent parameter which is the bulk quadrupolar hyperpolarizability α_{3B}.

Alternatively, if we apply the electric field gradient in Eq. (4) we will obtain [17]:

$$P_i(2\omega) = \chi_{ijkl} E_j(-ic\kappa_k) E_l \tag{9}$$

where c is a constant, and $i = \sqrt{-1}$ and κ_k is the component of the incident wave vector, inside the material. Thus, for the case of normal incidence $\vec{\kappa} = -\hat{k}$. Hence, $\vec{\kappa}$ only has a component in the z direction and then $\kappa_z = 1$. When this term is contracted

with the tensor, the results is

$$\overleftrightarrow{\chi}_{eff}^{(3B)}(001) = \frac{8ic\alpha_{3B}}{9V}\begin{pmatrix}\begin{pmatrix}0&0&1\\0&0&0\\1&0&0\end{pmatrix}\\\begin{pmatrix}0&0&0\\0&0&1\\0&1&0\end{pmatrix}\\\begin{pmatrix}1&0&0\\0&1&0\\0&0&1\end{pmatrix}\end{pmatrix} \tag{10}$$

which has a similar form to the tensor that describes the surface in the Si(001) direction and corresponds to a C_{2v} point-group symmetry [14]. This implies that when the gradient is normal to the surface, the effective third-rank tensor after contracting the result with the field gradient is identical to the nonlinear susceptibility that describes the surface of the crystal. The same result is obtained for the Electric-Field-Induced Second-Harmonic-Generation (EFISH) case when the DC field is in the same direction as that of incoming light that is directed normal to the surface [18]. Therefore, it is very difficult to separate the normal contribution of the quadrupolar SHG signal with the SHG contribution originating from the silicon surface. However, for an oblique incoming light incidence the case is different. Due to Snell's law, differences in the surface and bulk refractive index will result in a slightly different light propagation angle.

3.2. Si(111) Facet

Here we are going to generate the third order susceptibility tensor for a Si(111) facet orientation which according to the SBHM

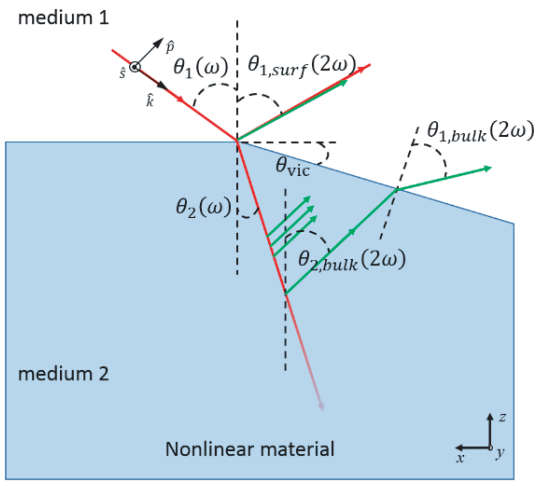

FIGURE 1. Proposal for separating contributions from the surface and bulk to SHG.

has the corresponding bond unit vectors [10]:

$$\hat{b}_1 = \begin{pmatrix}0\\0\\1\end{pmatrix}, \quad \hat{b}_2 = \begin{pmatrix}\sin\beta\\0\\\cos\beta\end{pmatrix},$$
$$\hat{b}_3 = \begin{pmatrix}-\frac{1}{2}\sin\beta\\\frac{\sqrt{3}}{2}\sin\beta\\\cos\beta\end{pmatrix}, \quad \hat{b}_4 = \begin{pmatrix}-\frac{1}{2}\sin\beta\\-\frac{\sqrt{3}}{2}\sin\beta\\\cos\beta\end{pmatrix} \tag{11}$$

using Eq. (5), evaluating the angle β, and fixing $\phi = \pi/2$, the susceptibility tensor for the quadrupolar contribution in the direction Si(111) is

$$\overleftrightarrow{\chi}^{(3B)} = \frac{4\alpha_{3B}}{27V}$$
$$\begin{pmatrix}\begin{pmatrix}6&0&0\\0&2&\sqrt{2}\\\sqrt{2}&0&1\end{pmatrix} & \begin{pmatrix}0&2&\sqrt{2}\\2&0&0\\\sqrt{2}&0&0\end{pmatrix} & \begin{pmatrix}0&\sqrt{2}&1\\\sqrt{2}&0&0\\1&0&0\end{pmatrix}\\\begin{pmatrix}0&2&\sqrt{2}\\2&0&0\\\sqrt{2}&0&0\end{pmatrix} & \begin{pmatrix}2&0&0\\0&6&-\sqrt{2}\\-\sqrt{2}&0&1\end{pmatrix} & \begin{pmatrix}\sqrt{2}&0&0\\0&-\sqrt{2}&1\\0&1&0\end{pmatrix}\\\begin{pmatrix}0&\sqrt{2}&1\\\sqrt{2}&0&0\\1&0&0\end{pmatrix} & \begin{pmatrix}\sqrt{2}&0&0\\0&-\sqrt{2}&1\\0&1&0\end{pmatrix} & \begin{pmatrix}1&0&0\\0&1&0\\0&0&7\end{pmatrix}\end{pmatrix}, \tag{12}$$

In analogy with the previous case, we can now contract this tensor Eq. (12) with the wavevector inside the material and normal to the surface, this is, $\vec{\kappa} = -\hat{k}$. Therefore

$$\overleftrightarrow{\chi}_{eff}^{(3B)}(111) = \frac{4ic\alpha_{3B}}{27V}\begin{pmatrix}\begin{pmatrix}0&\sqrt{2}&1\\\sqrt{2}&0&0\\1&0&0\end{pmatrix}\\\begin{pmatrix}\sqrt{2}&0&0\\0&-\sqrt{2}&1\\0&1&0\end{pmatrix}\\\begin{pmatrix}1&0&0\\0&1&0\\0&0&7\end{pmatrix}\end{pmatrix} \tag{13}$$

which is an effective third-rank tensor belonging to the C_{3v} point-group symmetry. This result is similar to our previous analysis, in the sense that the Si(111) surface also has a C_{3v} symmetry and the effective third-rank tensor takes a similar form as in EFISH when the DC field is applied normal to the surface [18]. The physical mechanisms that generate SHG are very different from those of surface, EFISH, and the gradient of the excited electric field, but the break of symmetry in the crystal occurs in the same direction in all these cases. The same analogy should apply to other nonlinear phenomena, such as bulk dipoles due to the absorption of the incoming electric field and spatial dispersion [21]. Therefore, mathematically, there is no difference because the tensor that describes the bulk of the crystal contains all the information about the symmetries present in that crystal. When the contraction of the full tensor with the vector representing the break of symmetry occurs,

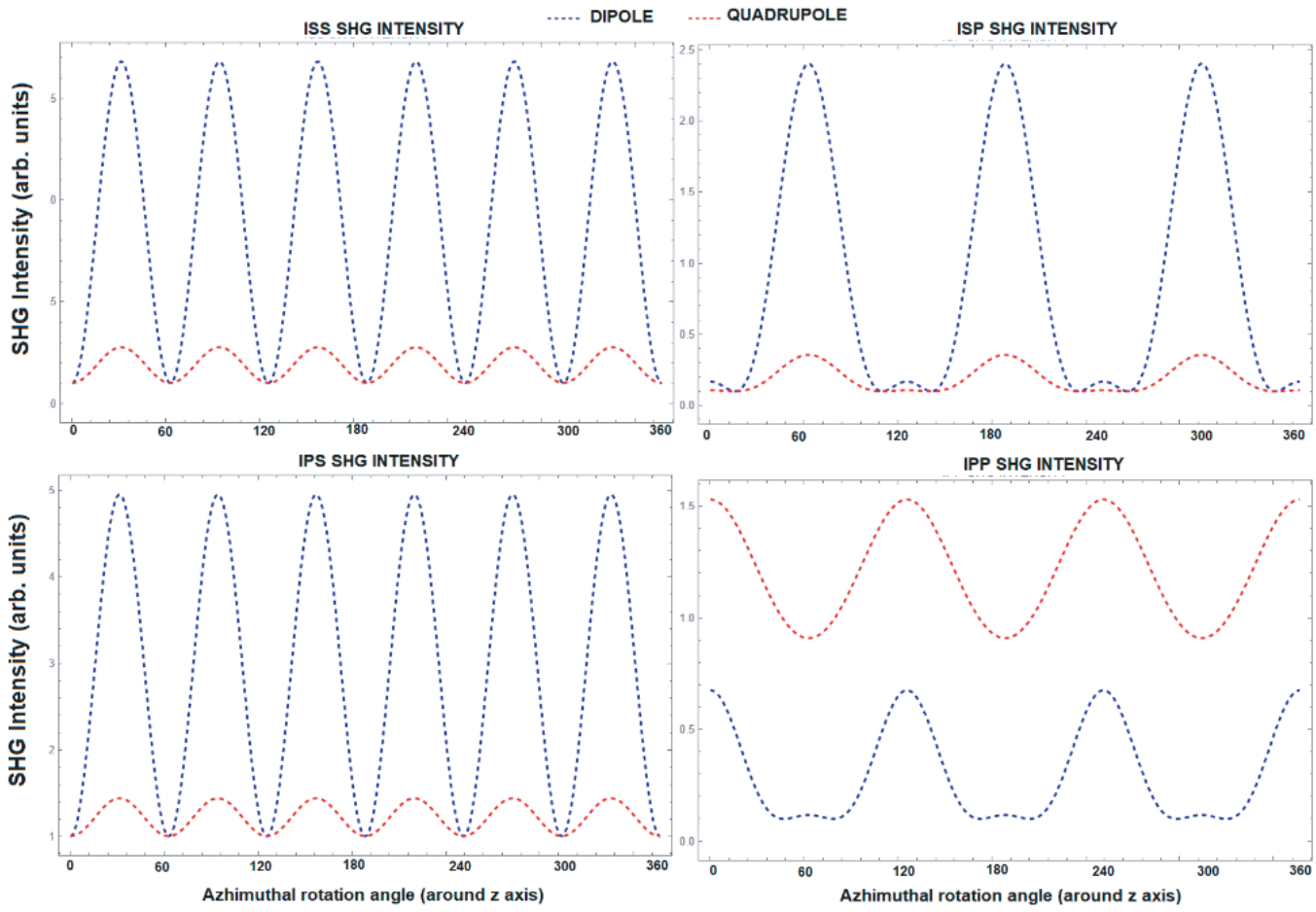

FIGURE 2. SBHM simulation of dipole and quadrupole SHG contribution for a Si(111) incidence = outgoing angle = 45°.

all the other symmetries disappear, and only the corresponding subset of symmetries remains, which is not affected by the break of symmetry in this particular direction.

Finally, we propose an experimental design to further distinguish the surface and bulk SHG sources, assuming a non-normal incidence-outgoing angle. The key here is generating a semi-vicinal surface where the incoming fundamental light is directed towards the flat surface and generating an outgoing light at a similar angle based on the law of reflection. However, the SHG light that propagates from within the bulk will be directed towards the vicinal surface where there is no incoming light. The interesting feature of such a surface geometry is the possibility to detect both the surface and bulk SHG using separate detectors placed at different angles. This idea is sketched in Fig. 1.

As can be seen in Fig. 1, the green arrow almost superimposed over the red arrow denotes the direction of the surface nonlinear contribution whereas the green arrow in the vicinal cut denotes the direction of the bulk nonlinear contributions, and we encourage experimental RASHG measurements using this design.

Figures 2 and 3 are the results of SBHM simulations for a Si(111) facet two different SHG outgoing angles, one at 45° (flat surface outgoing) and the other at 9.8° (vicinal surface outgoing), with a vicinal angle of 5°. We take as an example the Si(111) facet since for the Si(001) facet, our SBHM simulation provides similar patterns for the flat and vicinal outgoing angles only differing in their arbitrary intensity. The angle of 9.8° is derived based on geometrical calculations and Snell's law, considering the refractive index of silicon as described in the reference by Aspnes and Studna [30]. The differences between the angles are more apparent in the *pp* SHG polarization where for a flat surface the SHG surface contribution is threefold whereas for the vicinal surface the SHG contribution is from within the bulk and is given by a sixfold intensity feature. Thus in Fig. 3, the dipole contributions must be attributed to spatial dispersion. If the RASHG experiment results align with the SBHM predictions in Fig. 2 and Fig. 3, it indicates the presence of spatial dispersion which is simply a bulk dipolar contribution due to the decaying electric field. A precise high-small peak ratio value using RASHG experiment will furthermore determine the ratio of the spatial dispersion and quadrupolar contributions. Therefore, using this particular semi-vicinal surface allows us to convincingly distinguish between bulk and surface contributions for the first time as well as obtain the magnitude of these contributions and solve the longstanding debate

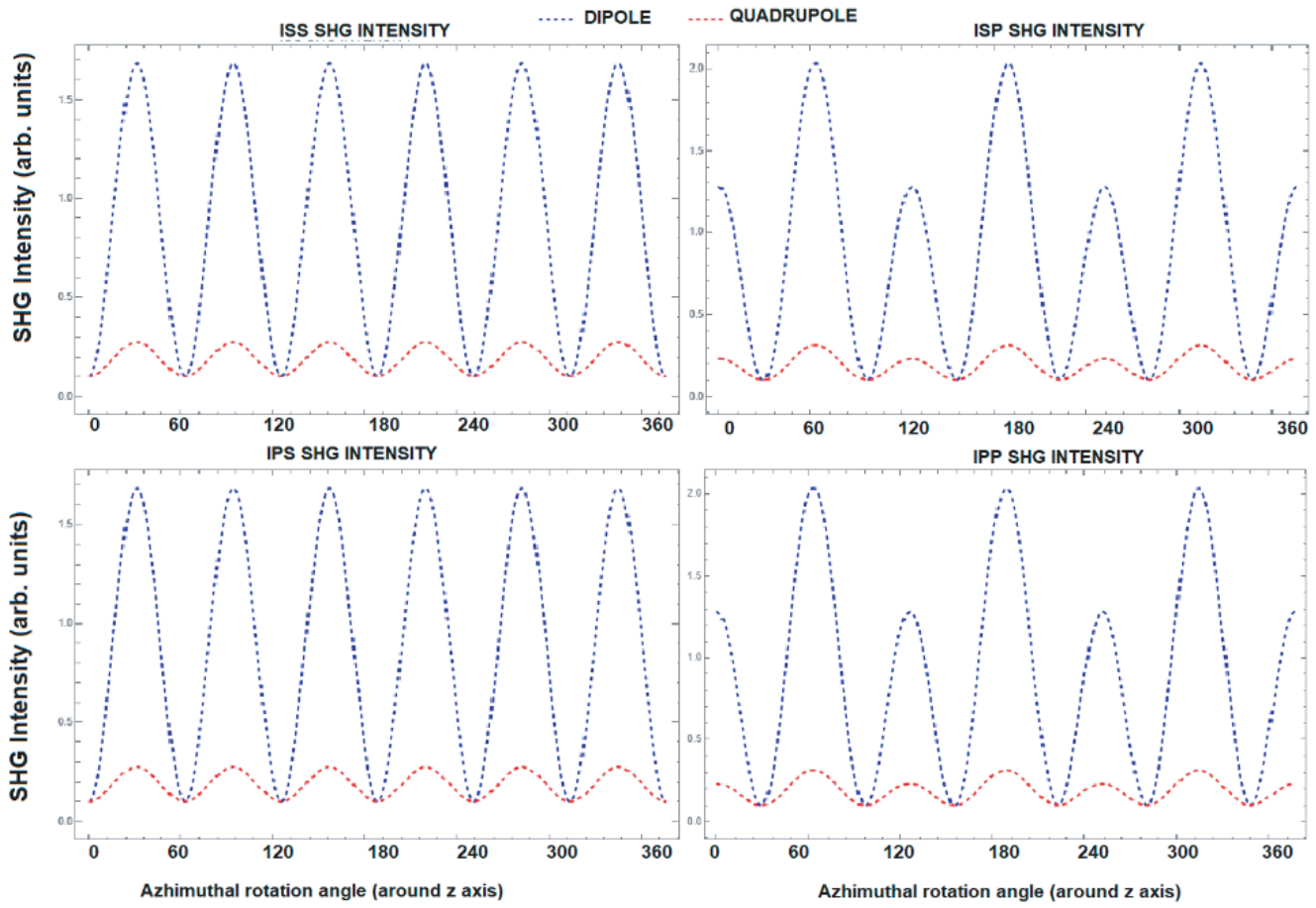

FIGURE 3. SBHM simulation of dipole and quadrupole SHG contribution for a Si(111) incidence $= 45°$ outgoing angle $= 9.81°$.

of the various SHG sources in silicon. Finally, we would like to emphasize that such a semi-vicinal surface SBHM analysis can also be performed to measure the surface and bulk contribution of other semiconductors such as GaAs, ZnO, and even perovskite structures whose bond vectors have already been determined in other works, e.g., see [22, 28, 31]. We invite experimenters to test our RASHG SHG intensity prediction.

4. CONCLUSIONS

We have investigated the third-order nonlinear phenomenon involving the bulk quadrupolar contribution to second harmonic generation (SHG) in centrosymmetric crystals for Si(001) and Si(111) facet orientations. Our analysis of the nonlinear tensor shows that for an incoming light beam normal to the surface, the generated quadrupolar response is identical to that produced by the surface when the contribution of the electric field gradient is included. This makes it difficult to separately identify surface and bulk SHG contributions. In other words, it is not possible to distinguish the bulk contribution from the surface-generated contribution under normal incidence. However, for a non-normal (oblique) incidence light beam, it is possible to isolate the quadrupolar contribution from the SHG signal originating from the crystal surface and the SHG signal generated within the bulk. Specifically, if Fresnel's coefficients are significant, creating a vicinal cut in the crystal with the excitation field impinging near the edge of the cut allows for differentiation of these two sources. Our numerical simulations for the semi-vicinal Si(111) facet with a vicinal angle of 5° show that the RASHG SHG intensity profiles from the surface and bulk can be distinguished, especially for the pp-SHG polarization. Additionally, these simulations enable us to determine the magnitude of the various SHG sources, providing a more comprehensive understanding of the contributions from both surface and bulk origins.

ACKNOWLEDGEMENT

H. H. thanks to Dana Abadi Perguruan Tinggi-Lembaga Pengelola Dana Pendidikan (DAPT-LPDP) through National Research Collaboration Funding Program (Riset Kolaborasi Nasional) with Grant No. 492/IT3.D10/PT.01.03/P/B/2023.

REFERENCES

[1] Franken, P. A., A. E. Hill, C. W. Peters, and G. Weinreich, "Generation of optical harmonics," *Physical Review Letters*, Vol. 7, No. 4, 118, 1961.

[2] Maiman, T. H., "Stimulated optical radiation in ruby," *Nature*, Vol. 187, 493–494, 1960.

[3] Bloembergen, N. and P. S. Pershan, "Light waves at the boundary of nonlinear media," *Physical Review*, Vol. 128, No. 2, 606, 1962.

[4] Armstrong, J. A., N. Bloembergen, J. Ducuing, and P. S. Pershan, "Interactions between light waves in a nonlinear dielectric," *Physical Review*, Vol. 127, No. 6, 1918, 1962.

[5] Maker, P. D. and R. W. Terhune, "Study of optical effects due to an induced polarization third order in the electric field strength," *Physical Review*, Vol. 137, No. 3A, A801, 1965.

[6] Ward, J. F. and G. H. C. New, "Optical third harmonic generation in gases by a focused laser beam," *Physical Review*, Vol. 185, No. 1, 57, 1969.

[7] Mendoza, B. S. and W. L. Mochán, "Polarizable-bond model for second-harmonic generation," *Physical Review B*, Vol. 55, No. 4, 2489, 1997.

[8] Arzate, N. and B. S. Mendoza, "Polarizable bond model for optical spectra of Si (100) reconstructed surfaces," *Physical Review B*, Vol. 63, No. 11, 113303, 2001.

[9] Aspnes, D. E., "Bond models in linear and nonlinear optics," in *Ultrafast Nonlinear Imaging and Spectroscopy III*, Vol. 9584, 21–31, 2015.

[10] Powell, G. D., J.-F. Wang, and D. E. Aspnes, "Simplified bond-hyperpolarizability model of second harmonic generation," *Physical Review B*, Vol. 65, No. 20, 205320, 2002.

[11] Wang, J.-F. T., G. D. Powell, R. S. Johnson, G. Lucovsky, and D. E. Aspnes, "Simplified bond-hyperpolarizability model of second harmonic generation: Application to Si-dielectric interfaces," *Journal of Vacuum Science & Technology B*, Vol. 20, No. 4, 1699–1705, 2002.

[12] McGilp, J. F., "Using steps at the Si–SiO_2 interface to test simple bond models of the optical second-harmonic response," *Journal of Physics: Condensed Matter*, Vol. 19, No. 1, 016006, 2007.

[13] Hardhienata, H., A. Prylepa, D. Stifter, and K. Hingerl, "Simplified bond-hyperpolarizability model of second-harmonic-generation in Si (111): Theory and experiment," in *Journal of Physics: Conference Series*, Vol. 423, No. 1, 012046, 2013.

[14] Alejo-Molina, A., H. Hardhienata, and K. Hingerl, "Simplified bond-hyperpolarizability model of second harmonic generation, group theory, and Neumann's principle," *Journal of the Optical Society of America B*, Vol. 31, No. 3, 526–533, 2014.

[15] Alejo-Molina, A., K. Hingerl, and H. Hardhienata, "Model of third harmonic generation and electric field induced optical second harmonic using simplified bond-hyperpolarizability model," *Journal of the Optical Society of America B*, Vol. 32, No. 4, 562–570, 2015.

[16] Hardhienata, H., A. Alejo-Molina, C. Reitböck, A. Prylepa, D. Stifter, and K. Hingerl, "Bulk dipolar contribution to second-harmonic generation in zincblende," *Journal of the Optical Society of America B*, Vol. 33, No. 2, 195–201, 2016.

[17] Reitböck, C., D. Stifter, A. Alejo-Molina, K. Hingerl, and H. Hardhienata, "Bulk quadrupole and interface dipole contribution for second harmonic generation in Si (111)," *Journal of Optics*, Vol. 18, No. 3, 035501, 2016.

[18] Alejo-Molina, A., H. Hardhienata, P. A. Márquez-Aguilar, and K. Hingerl, "Facet-dependent electric-field-induced second harmonic generation in silicon and zincblende," *Journal of the Optical Society of America B*, Vol. 34, No. 6, 1107–1114, 2017.

[19] Reitböck, C., D. Stifter, A. Alejo-Molina, H. Hardhienata, and K. Hingerl, "Nonlinear ellipsometry of Si (111) by second harmonic generation," *Applied Surface Science*, Vol. 421, 761–765, 2017.

[20] Hardhienata, H., T. I. Sumaryada, B. Pesendorfer, and A. Alejo-Molina, "Bond model of second-and third-harmonic generation in body-and face-centered crystal structures," *Advances in Materials Science and Engineering*, Vol. 2018, No. 1, 7153247, 2018.

[21] Hardhienata, H., A. Alejo-Molina, M. D. Birowosuto, A. Baghbanpourasl, and H. Alatas, "Spatial dispersion contribution to second harmonic generation in inversion-symmetric materials," *Physical Review B*, Vol. 103, No. 12, 125410, 2021.

[22] Hardhienata, H., S. Faci, A. Alejo-Molina, M. R. Priatama, H. Alatas, and M. D. Birowosuto, "Quo vadis nonlinear optics? An alternative and simple approach to third rank tensors in semiconductors," *Symmetry*, Vol. 14, No. 1, 127, 2022.

[23] Chen, W.-T., T.-Y. Yen, Y.-H. Hung, and K.-Y. Lo, "Structure of an in situ phosphorus-doped silicon ultrathin film analyzed using second harmonic generation and simplified bond-hyperpolarizability model," *Nanomaterials*, Vol. 12, No. 23, 4307, 2022.

[24] Chen, W.-T., T.-Y. Yen, Y.-H. Hung, Y.-H. Huang, S.-J. Chiu, and K.-Y. Lo, "Second harmonic generation and simplified bond hyperpolarizability model analyses on the intermixing of Si/SiGe stacked multilayers for gate-all-around structure," *Nanotechnology*, Vol. 34, No. 14, 145702, 2023.

[25] Bloembergen, N., R. K. Chang, S. S. Jha, and C. H. Lee, "Optical second-harmonic generation in reflection from media with inversion symmetry," *Physical Review*, Vol. 174, No. 3, 813, 1968.

[26] Bauer, K.-D., M. Panholzer, and K. Hingerl, "Bulk quadrupole contribution to second harmonic generation from a microscopic response function," *Physica Status Solidi (B)*, Vol. 253, No. 2, 234–240, 2016.

[27] Bauer, K.-D. and K. Hingerl, "Bulk quadrupole contribution to second harmonic generation from classical oscillator model in silicon," *Optics Express*, Vol. 25, No. 22, 26 567–26 580, 2017.

[28] Hardhienata, H., I. Priyadi, H. Alatas, M. D. Birowosuto, and P. Coquet, "Bond model of second-harmonic generation in wurtzite ZnO (0002) structures with twin boundaries," *Journal of the Optical Society of America B*, Vol. 36, No. 4, 1127–1137, 2019.

[29] Boyd, R. W., *Nonlinear Optics*, Academic Press, 2003.

[30] Aspnes, D. E. and A. A. Studna, "Dielectric functions and optical parameters of Si, Ge, GaP, GaAs, GaSb, InP, InAs, and InSb from 1.5 to 6.0 eV," *Physical Review B*, Vol. 27, No. 2, 985, 1983.

[31] Hardhienata, H., H. A. Kharfan, S. Faci, M. D. Birowosuto, and H. Alatas, "Bond model of second harmonic generation in tetragonal and orthorhombic perovskite structures," *Journal of the Optical Society of America B*, Vol. 40, No. 11, 2773–2781, 2023.